

43 1. Introduction

44 The Mediterranean Sea is a biodiversity hotspot, representing 4 to 18% of global marine species (Bianchi
45 & Morri, 2000). This reservoir has been under increasing pressure for several decades due to habitat
46 degradation, marine and atmospheric pollution, invasive species, and climate change. Fishing is a major
47 activity in the Mediterranean Sea, with catches reaching 1.19 million tons in total in 2020. The majority
48 of fisheries are industrial, with an annual catch of 1 million tons. Yet, this activity represents only 17%
49 of the total number of boats, with the remaining 83% engaged in artisanal fishing (FAO, 2020). The lack
50 of regulation of artisanal vessels, illicit fishing practices, the discard of unwanted catch, and the
51 overfishing of fish stocks have collectively led to the overexploitation of marine resources and an
52 irreversible decline in fish stocks (Carlson et al., 2016; Zaimen et al., 2021). Besides, the majority of
53 specific fish stocks have not yet been assessed, making it difficult for political decision-makers to apply
54 and establish regulations (Marengo et al., 2016). As a locally important fishing resource, the
55 Mediterranean spinous spider crab *Maja squinado* (Herbst, 1788) has experienced a significant decline
56 in its population in recent years, likely due to overexploitation (Abello et al., 2014; Durán et al., 2013;
57 Martín et al., 2012; Rotllant et al., 2014).

58 In areas such as the Balearic Islands or the Columbretes Islands, the species appears to be nearly extinct
59 for approximately a decade, prompting research and reintroduction initiatives (Garcia, 2007; Torres et
60 al., 2013). Given this decrease in stocks, *Maja squinado* is internationally recognised as a species of
61 ecological interest within the United Nations Environment Programme's Action Plan for the
62 Mediterranean (UNEP/MAP). Additionally, it was included as a protected species in the Bern
63 Convention for the Conservation of European Wildlife and Natural Habitats and was added to Appendix
64 III of the Barcelona Convention in 2009. In France, the IUCN has not yet concluded on the species'
65 status, however regional decrees are already applied in order to limit and regulate catches by recreational
66 fishing. In Corsica, populations continue to support exploitation by small-scale fisheries (Bousquet et
67 al., 2022) but, a notable decline in CPUEs (Catches per unit effort) has been observed in recent years
68 (Marengo et al., 2023).

69 The spinous spider crab *Maja squinado*, a member of the Majidae family, was initially described as
70 inhabiting both the Atlantic and the Mediterranean Sea. In 1998, Neumann proposed a distinction
71 between *Maja squinado* and *Maja brachydactyla* (Balss, 1922) based on morphological characteristics
72 identified by Balss in 1922, with the respective distribution areas assigned to the Mediterranean and the
73 Atlantic (Neumann, 1998). This differentiation was further supported by a genetic study that analyzed
74 mitochondrial gene variations in Atlantic (*Maja brachydactyla*) and Mediterranean (*Maja squinado* and
75 *Maja crispata*) spider crab populations (Sotelo et al., 2008). Given that a significant proportion of the
76 studies conducted on *Maja squinado* were, in fact, based on the Atlantic species *Maja brachydactyla*,
77 our understanding of the biology of *Maja squinado* in the Mediterranean is somewhat limited and varies

78 according to different authors and geographic areas. Nevertheless, studies consistently agreed that these
79 crabs undertake seasonal migrations, descending to depths of up to 150 meters in winter and ascending
80 to shallower waters (10 to 15 m) in summer (Gualtieri et al., 2013; Rotllant et al., 2015). Mating typically
81 occurs during the autumn migration. Gravid females, those carrying at least fertilized eggs, ascend in
82 summer to spawn, while males remain at deeper levels. These females possess a spermatheca, enabling
83 them to spawn multiple times from winter matings. The number of egg clutches and larvae varies
84 according to authors, geographical areas, and water temperatures. Each female produces approximately
85 three clutches of 30,000 to 200,000 larvae (Calado et al., 2013; Durán et al., 2012). Gravid females
86 incubate the eggs under their abdomen before releasing the larvae at the zoea I stage, which then progress
87 through three stages: zoea I (ZI), zoea II (ZII), and megalopa. *Maja squinado* eggs and larvae are carried
88 by currents and drift in the environment to complete their lifecycle, a process known as larval dispersion
89 (Okubo, 1994). This process involves biological and physical mechanisms that facilitate the movement
90 of larvae from breeding to recruitment sites (Begon et al., 2005). Hence, the transport of larvae is
91 influenced by physical oceanic factors such as currents and turbulence (Power, 1984). In addition, larval
92 behaviours, such as larval vertical migration or free swimming, also play a role in dispersal (Adams et
93 al., 2012; Gary et al., 2020). On a larger scale, exchanges between subpopulations are vital for
94 understanding larval connectivity and the state and connections between marine metapopulations
95 (Pineda et al., 2007).

96 Understanding the population dynamics of *Maja squinado* is crucial for developing effective
97 management and conservation strategies. Although biophysical models are not often used for population
98 dynamics, they are frequently employed to investigate pelagic larval dispersal and connectivity (Swearer
99 et al., 2019). By integrating biophysical modeling, we can gain insights into the species' larval stages,
100 aiding in the prediction of dispersal patterns and connectivity, which are essential for informed
101 management and conservation efforts. This approach offers numerous benefits for predicting and
102 visualising the dynamics of population dispersal and for hypothesising species vulnerabilities. For
103 example, it can highlight isolated habitats or a lack of connectivity between populations, which are
104 critical for effective conservation strategies (Jahnke & Jonsson, 2022; Lett et al., 2010). Individual-
105 based models (IBMs) are designed to include detailed information about the life history traits of species
106 for which researchers intend to model spatial and/or temporal dynamics (DeAngelis & Mooij, 2005).
107 Each individual in the model is defined by a set of state variables and behaviours, which are determined
108 according to available information on the species and the model's desired level of precision. These
109 include geographical location, physiological traits, and certain behavioural traits such as reproduction
110 and habitat selection. In a biophysical model, the trajectories of particles representing larvae are
111 influenced by ocean currents and other environmental factors. By incorporating larval behaviours and
112 physiological processes, the model becomes more precise, allowing for refined predictions that align
113 more closely with other scientific approaches studying the species of interest.

114 In many Brachyura species, larval dispersion and migration are influenced by dominant ocean currents,
115 as well as seasonal variations, water temperature, and food availability (Anger et al., 2015; Anger, 1991;
116 Bryars & Havenhand, 2006; Epifanio & Garvine, 2001b). Significant environmental shifts in the
117 Mediterranean were observed in 2014, particularly in the Northwestern region, with increased
118 temperature and salinity, contrasting with a decline in these parameters in the offshore Ligurian
119 Levantine Intermediate Water (LIW) during the same period (Margirier et al., 2020). This marked the
120 start of an accelerated warming trend in the Mediterranean Sea (Margirier et al., 2020; Pastor et al.,
121 2020), reflecting global patterns (Yin et al., 2018).

122 *Maja squinado* has significantly declined in some Mediterranean areas, such as the Balearics, but
123 continues to be exploited in others, like Corsica, despite its "non-evaluated" IUCN status. The species'
124 ecology and population dynamics remain poorly understood, posing challenges for future predictions.
125 Biophysical modeling, however, offers valuable insights into larval dispersal and connectivity. This
126 study investigates the dispersal trajectories of *Maja squinado* larvae in the Mediterranean from 2010 to
127 2020, focusing on connectivity between spawning and nursery areas and analysing changes over time
128 and environmental variations.

129

130 **2. Material and Methods**

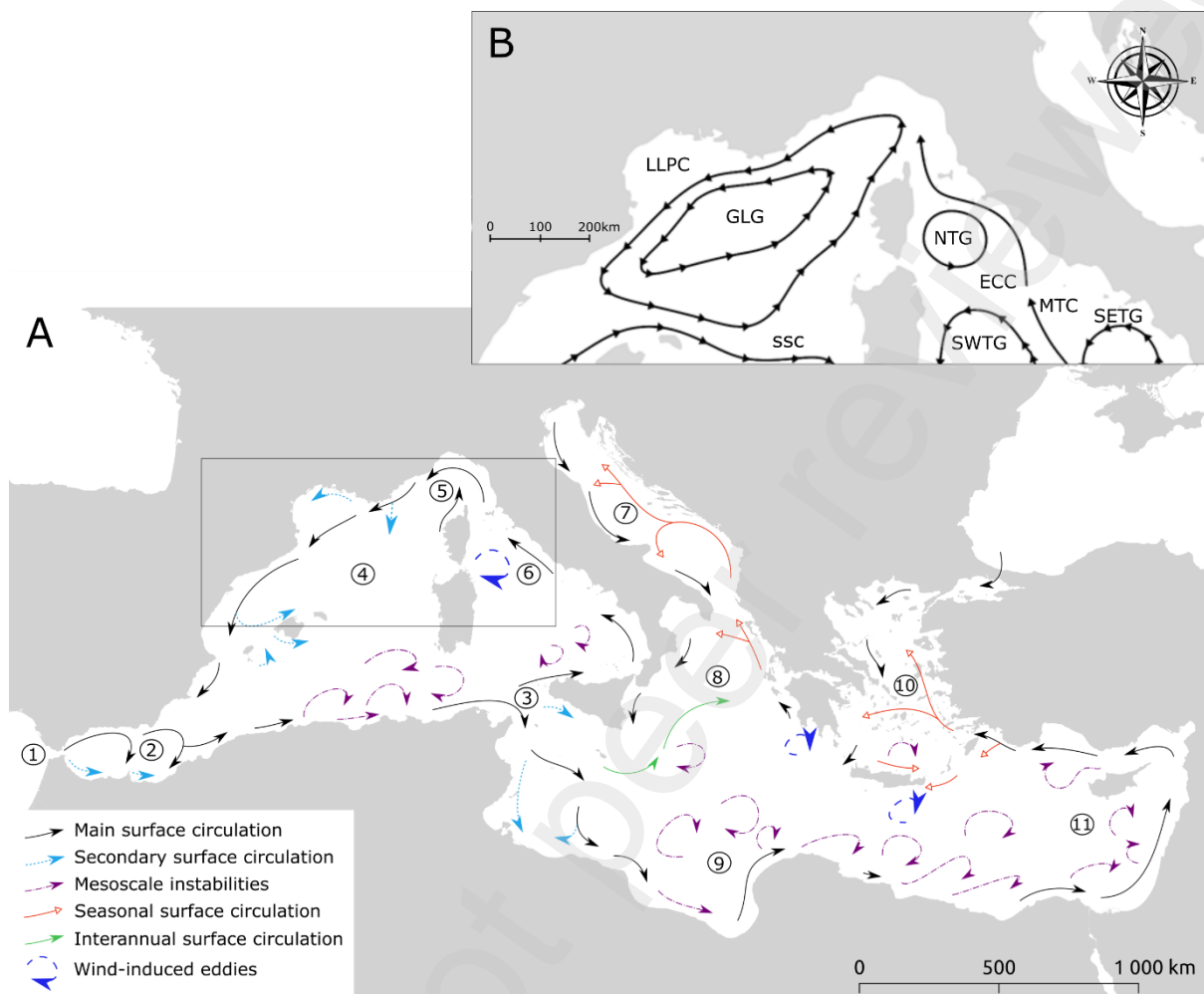
131

132 **2.1 Mediterranean's surface circulation**

133 The Mediterranean Sea is divided into two main basins, the Western and Eastern, separated by the Sicily-
134 Tunisia Strait. The Western Basin extends from the Alboran Sea to the Tyrrhenian Sea, with the Atlantic
135 Ocean connected to it via the Strait of Gibraltar. The Eastern Basin extends from the Adriatic to the
136 Levantine Sea, including the Ionian and Libyan Seas. The Mediterranean Sea's intricate surface
137 circulation, influenced by its segmented geography and complex seabed, predominantly exhibits
138 anticyclonic movement. Fresh Atlantic waters enter the Mediterranean through the Strait of Gibraltar,
139 increasing in density due to evaporation before exiting, typically taking 50 to 100 years to circulate.
140 Surface currents are influenced by wind and topography, forming stable gyres and up to one-kilometre-
141 wide eddies. However, some areas exhibit instabilities over time (Millot & Taupier-Letage, 2005;
142 Pinardi et al., 2015) (Fig. 1A).

143 Surface currents in the northwestern Mediterranean are primarily influenced by thermohaline
144 circulation, with cyclonic currents observed near the continental slopes. Notable currents include the
145 Liguro-Provençal-Catalan Current, which flows in an east-to-west direction, and various gyres such as
146 the Gulf of Lion Gyre and the Northern Tyrrhenian Gyre, which exhibit distinct circulatory patterns.
147 Furthermore, the Tyrrhenian Sea's connectivity with the Corsican and Sardinian shores is characterised

148 by the presence of various currents and gyres, which collectively contribute to the formation of a
149 dynamic marine environment (Pinardi et al., 2015) (Fig. 1B).



150

151 Figure 1: **Map of the general circulation currents in the Mediterranean (A)**, covering all basins (adapted from
152 Millot and Taupier-Letage, 2005). 1: Strait of Gibraltar, 2: Alboran Sea, 3: Sicilia-Tunisia Strait, 4: Algero-
153 Provençal Basin, 5: Ligurian Sea, 6: Tyrrhenian Sea, 7: Adriatic Sea, 8: Ionian Sea, 9: Libyan Sea, 10: Aegean
154 Sea, 11: Levantine Sea. **Focus on the Northwestern Mediterranean Sea (B)** adapted from the study by Pinardi
155 et al. (2015). LLPC: Liguro-Provençal-Catalan Current, GLG: Gulf of Lion Gyre, NTG: Northern Tyrrhenian
156 Gyre, ECC: Eastern Corsica Current, SSC: Southern Sardinia Current, MTC: Middle Tyrrhenian Current, and
157 SETG: South-Eastern Tyrrhenian Gyre.

158

159 2.2 Hydrodynamical models

160 The simulations for this study were performed using two hydrodynamic models. The first one,
161 MEDSEA_MULTIYEAR_PHY_006_004 (MedMFC), was used to carry out simulations encompassing
162 the entirety of particle release polygons representing larvae in the Western Mediterranean. This model,
163 which presents a daily temporal resolution, integrates a hydrodynamic model contributed by the Nucleus
164 for European Modelling of the Ocean (NEMO). It is further enhanced by a variational data assimilation
165 approach known as OceanVAR, which processes vertical profiles of temperature and salinity, along

166 with satellite-derived sea level anomaly data. The dataset includes a comprehensive reanalysis segment,
167 as well as an interim segment that extends from the end of the reanalysis to one month prior to the
168 current date. The model operates on a finely calibrated horizontal grid with a resolution of $1/24^\circ$,
169 equivalent to approximately 4-5 km (Escudier et al., 2021). A second hydrodynamic model,
170 MARS3DMed, was employed for focused analyses and to attempt observing phenomena at a finer scale.
171 This model, derived from the MARS3D (Model for Application at Regional Scales 3D) code and
172 developed by Ifremer, has a temporal resolution of three hours, a horizontal resolution of about 1.2
173 kilometers, and 60 vertical levels using a generalized sigma coordinate system on an Arakawa-C grid,
174 extending from the seabed to the surface, and is adapted for fine graphical resolutions (Arakawa &
175 Lamb, 1977; Lazure & Dumas, 2008).

176

177 **2.3 The Lagrangian transport tool**

178 The model employed for larval dispersal is Ichthyop v.3.3.16, an offline Java Lagrangian tool (Lett et
179 al., 2008). This tool has been extensively utilised in marine ecology studies, including those by Rojas-
180 Araos et al. (2024) and Flores-Valiente et al. (2023), as well as in the broader field of physical
181 oceanography, including work by Al-Qattan et al. (2023) and de Mello et al. (2023). This model is
182 biophysical as it assesses the influence of physical and biological factors on the dynamics of
183 ichthyoplankton. It follows the water masses or drifting entities from oceanic models ROMS, MARS,
184 NEMO, or SYMPHONIE (Imzilen et al., 2023). The particle trajectories are calculated using a fourth-
185 order Runge-Kutta method with a constant time step (van Sebille et al., 2018). The time step used in
186 time integration of motion was defined according to the Ichthyop configuration editor to ensure that the
187 Courant-Friedrichs-Lewy (CFL) condition is met, 720 seconds for the MARS3DMed outputs and 2880
188 seconds for the MedMFC outputs. Data recordings are made at regular intervals (every 60th and 15th
189 timestep for the respective models), capturing the position of the particles every 12 hours. Horizontal
190 diffusion was set according to the standard parameters of Ichthyop based on Peliz et al. (2007), with a
191 dissipation rate of $10^{-9} \text{ m}^2 \cdot \text{sec}^{-3}$, while vertical migration follows a daily cycle depending on the depth
192 and the sunrise and sunset times (Table 1). Buoyancy is added to the vertical velocity, determined by
193 the density differences between the egg and the water, depending on temperature and salinity (Table 1).
194 The particle release sub-model depends on the number, depth, and release dates, with parameters
195 assigned to specific sites (Table 1). Particle retention at these sites depends on the minimum number of
196 days before a particle can be considered as retained (Table 1). After this period, if a particle is found at
197 a site, it stops moving. If a particle exceeds a certain pelagic larval duration (PLD) and is not found at
198 any site, it is considered dead. The schedule for particle releases corresponds to spawning events for
199 *Maja squinado* in the Western Mediterranean as documented in the literature, particularly using data
200 available for Corsica and Catalonia (Calado et al., 2013, and Duran et al., 2012 in Corsica; Rotllant et
201 al., 2014 in Corsica and Catalonia). Thus, each simulation year includes eight release dates, as detailed

202 in Table 1. Each release site disperses 40,000 particles at depths ranging from 0m to 50m (Gualtieri et
 203 al., 2013). The maximum duration of particle dispersal is 20 days, and particles are considered as
 204 competent for settlement from 17 days, corresponding to the juvenile stage of *Maja squinado* (Durán et
 205 al., 2012; Rotllant et al., 2014). Each particle undergoes daily vertical migration at sunrise and sunset,
 206 within the depths defined by the photic zone at 1.10^{-7} m^{-2} for these larvae, averaging about 30 meters
 207 deep during the day and about 1 meter at night (Anger et al., 2015; Ospina-Alvarez et al., 2018). No
 208 horizontal migration or free swimming is included, as the swimming appendages of the early zoeae
 209 stages are primarily for vertical movement, before being replaced by walking and feeding appendages
 210 at the megalopa and first juvenile stages. The buoyancy of the particles is determined by a density of
 211 0.9 g/cm^3 (Epifanio & Garvine, 2001a). Finally, a rebound behavior upon contact with physical barriers
 212 is attributed to the particles, with a force equivalent to that required to overcome these barriers.
 213

214 Table 1. Biological parameters of the simulations applied to the dispersion of *Maja squinado*.

Parameter	Value	Reference
Pelagic larval duration (PLD)	20 days	Durán et al., 2012
Release date (per year)	April 15 - Start of the laying period. April 22 - One week after the start. April 29 - Two weeks after the start. May 6 - Three weeks after the start. May 13 - Four weeks after the start. May 20 - Five weeks after the start. May 27 - Six weeks after the start. May 31 - End of the laying period.	
Particles number	MedMFC: 50000 particles were released on each release day (8 days in total), amounting to 400000 particles per simulation. This equates to 4400000 particles over the 11-year study period, distributed evenly across 36 zones. MARS3DMed: in order to maintain proportional relationships, 31250 particles were released each day of the release period (8 days in total), resulting in a total of 250000 particles per simulation, or 2750000 particles over the 11-year study period, distributed evenly across 23 polygons in the Northwestern Mediterranean.	
Release depth	0 – 25m	Gualtieri et al., 2013
Release polygons	See Figure 2 for geographical localization: 1: MA1, 2: SP2, 3: SP5, 4: SP6, 5: SP7, 6: SP8, 7: SP9, 8: FR2, 9: FR3, 10: FR-I, 11: CApi, 12: NWCO The following codes correspond to the polygon numbers: 13: WCO, 14: SWCO, 15: SCO, 16: SECO, 17: NECO, 18: IT3, 19: IT4, 20: NSA, 21: NWSA, 22: SWSA, 23: SSA, 24: SESA, 25. The following abbreviations are used in this document:	Rotllant et al. 2014, Guerao & Rotllant 2010, Guerao et al. 2016, Seytre et al. 2013, Modena et al. 2001 and Durán et al. 2012 and grey littérature.

NESA, 26: IT7, 27: IT8, 28: IT9, 29: IT10, 30: SIC1, 31: SIC2, 32: USTi, 33: SIC3, 34: TUN, 35: AL3, 36: MA-AL.

Ideal habitat for recruitment polygons	See Figure 3 for geographical localization: 1:MA1, 2:ALB, 3:SP1, 4:SP2, 5:SP3, 6:SP4, 7:SP5, 8:SP6, 9:COLUI, 10:SP7, 11:BA2, 12:BA1, 13:BA3, 14:BA4, 15:BA8, 16:BA5, 17:SP8, 18:BA7, 19:SP9, 20:BA6, 21:SP-FR, 22:FR1, 23:FR2, 24:FR3, 25:FR4, 26:FR-I, 27:IT1, 28:CAPI, 29:NWCO, 30:WCO, 31:SWCO, 32:SCO, 33:SECO, 34:NECO, 35:IT2, 36:IT3, 37:PIAI, 38:IT4, 39:IT5, 40:NSA, 41:NWSA, 42:SWSA, 43:SSA, 44:SESA, 45:NESA, 46:IT6, 47:IT7, 48:IT8, 49:IT9, 50:IT10, 51:SIC1, 52:EOLI, 53:SIC2, 54:USTi, 55:SIC3, 56:TUN, 57:ALTUN, 58:GALI, 59:AL4, 60:AL3, 61:AL2, 62:AL1, 63:MA-AL.	Rotllant et al. 2014, Guerao & Rotllant 2010, Guerao et al. 2016, Seytre et al. 2013, Modena et al. 2001 and Durán et al. 2012 and grey littérature.
Minimum retention age	17 days	Rotllant et al., 2014
Buoyancy	0.9g/cm ³	Epifanio & Garvine, 2001a
Vertical migration depth	day: 30m – night: 1m	Ospina-Alvarez et al., 2018
Coastal particles behaviour	Bouncing	

215

216

2.4 Delimitation of release and recruitment sites

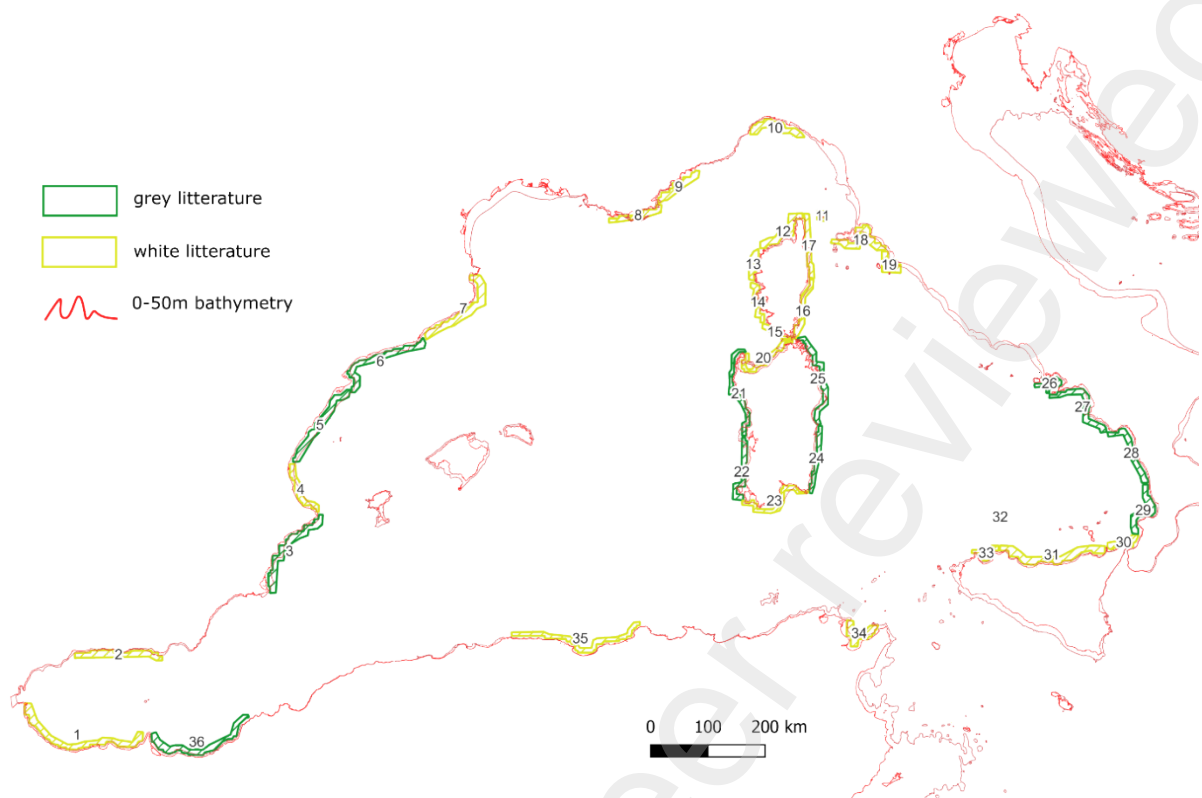
217 The sites used for the release of particles were designed based on the presence of *Maja squinado* as
 218 documented in the literature (Rotllant et al. 2014, Guerao & Rotllant 2010, Guerao et al. 2016, Seytre
 219 et al. 2013, Modena et al. 2001) Durán et al. 2012) Rotllant et al. 2015, Angeletti et al. 2014), Gualtieri
 220 et al. 2013, Durán et al. 2013, Calado et al. 2013, Sotelo et al. 2008, Vignoli et al. 2004) Rocklin 2010)
 221 Mura & Corda 2011, and Pipitone & Arculeo 2003; Fig. 2). Using the same body of literature, the
 222 recruitment sites were approximated by coastal areas in proximity to documented catch of *M. squinado*,
 223 taking into account bathymetry (< 50 m, Fig. 3).

224

225

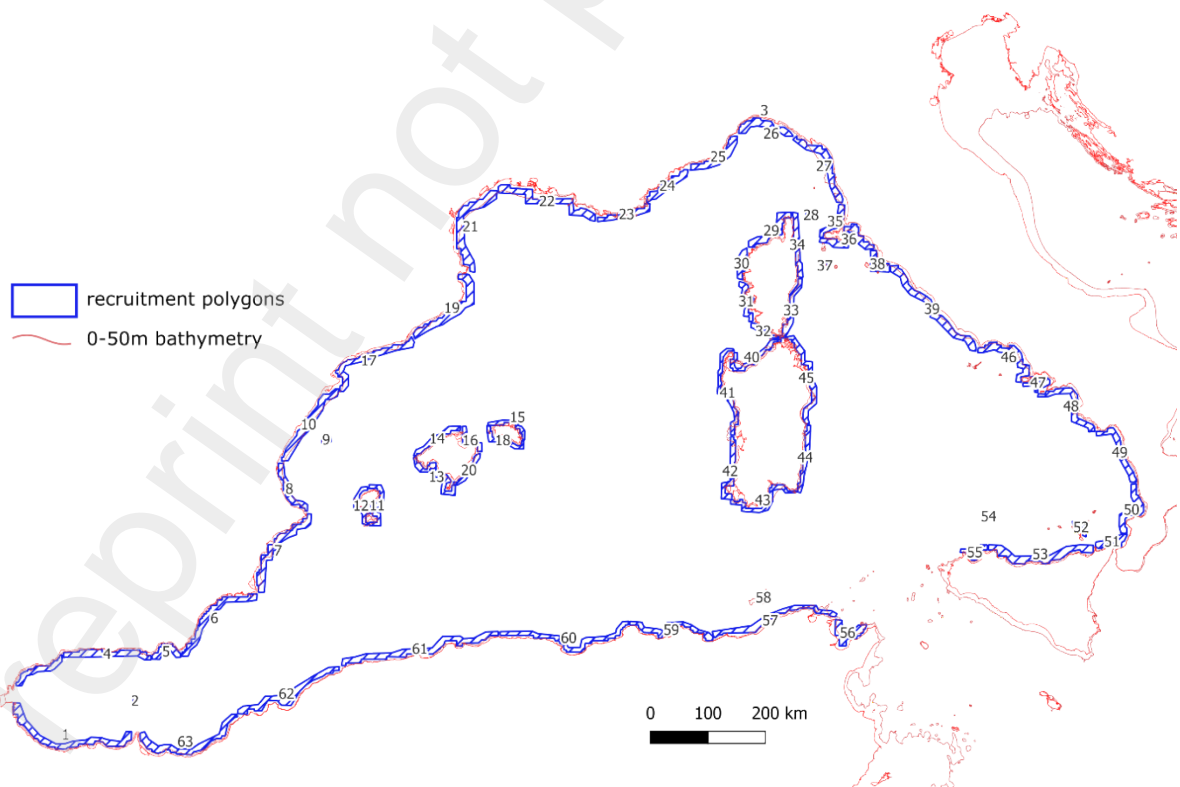
226

227



228

229 Figure 2: The 36 polygons used for particle release within the MedMFC model domain as identified in white (dark
 230 grey polygons) and grey (light green) literature. See Table 1 for the detailed names of the acronyms.



231

232 Figure 3: The 63 ideal habitat for recruitment polygons within the MedMFC model domain. See Table 1 for the
 233 detailed names of the acronyms.

234

2.5 Environmental trends visualization and data analysis

235 The Ichthyop simulation outputs are files in netcdf format, which were analyzed with R (version 4.0.4;
236 R Core Team 2021) and Python (version 3.11) scripts. Firstly, particle density maps were produced over
237 the entire period (2010-2020). Trajectory densities were calculated through the following steps: the final
238 positions of particles were extracted from simulation outputs. The coordinates (longitude and latitude)
239 of these particles were used to create spatial line objects, which were then converted into spatial vectors.
240 These vectors were rasterized onto a background map grid, where each raster cell contained the sum of
241 trajectories passing through that cell. Mathematically, this entails enumerating the number of particles
242 present in each grid cell at the conclusion of the simulation. A coefficient of variation (CV) was
243 calculated in each map in order to compare the relative variability between different trajectories or
244 periods, even if the absolute densities differ. Connectivity matrices between release zones and
245 recruitment zones, as well as local retention and self-recruitment at each site, and distribution of traveled
246 distances and directions followed from release to recruitment were also computed. On connectivity
247 matrices, a Gini coefficient (Hixon & Jones, 2005) was also shown on connectivity matrices in order to
248 assess disparities between years and sites.

249

250 The sea surface temperature data extracted from the Copernicus Marine Environment Monitoring
251 Service (CMEMS) satellite product over the western Mediterranean Sea demonstrated a temperature
252 increase trend of $0.034 \pm 0.002^\circ\text{C}$ per year, with a 95% confidence interval (Appendix Figure A1). To
253 analyse trends spatially and focus on the last decade, data from the MedMFC model were examined at
254 all points in the Western Mediterranean (focusing on our study window), providing a more spatially
255 detailed view of regional temperature variations. Linear regression was used to calculate a linear
256 temperature trend for each grid point, with a color gradient from blue (indicating a decrease in
257 temperature) to red (indicating an increase in temperature) used to map these trends. A comprehensive
258 examination of these findings is provided in the appendix section.

259

260 The simulation results were divided into two groups: 2010-2014 and 2015-2019, in order to contrast
261 periods of different average temperatures while maintaining an equal number of simulations for
262 comparison. Firstly, an overall visualization was carried out, with the calculation of KDE's (kernels
263 density estimates). The KDE calculation is based on a symmetric function centered around each data
264 point. The most commonly used kernel is the Gaussian kernel (normal function), which is selected based
265 on the bandwidth, which determines the extent of the smoothing. A smaller bandwidth leads to a more
266 detailed estimate, while a larger bandwidth results in a smoother estimate. In the context of particle
267 position simulations modelling larvae, KDE can be employed to estimate the spatial density of particle
268 positions at different times, thereby enabling the visualization of areas of high particle concentration
269 and the identification of any differences between the two scenarios. Secondly, a subsampling of two

270 zones was employed to analyse the distribution of travelled distances and directions followed from
271 release to recruitment. The distances were calculated using the Haversine formula, which accounts for
272 the Earth's curvature by calculating the great-circle distance between points. The presented plots
273 illustrate the distribution and density of data points, comparing the density of particles based on the
274 distance travelled from spawning areas in the pre- and post-warming scenarios of the Western
275 Mediterranean. Furthermore, wind roses were constructed to examine the typical orientations assumed
276 by the particles following their arrival at a recruitment zone for each year. The orientations were
277 calculated by determining the angle of each trajectory segment and averaging these angles, with the
278 weights being proportional to the distances.

279

280 3. Results

281

282

28

28

28

28

28

28

28

28

28

28

28

28

28

28

28

28

28

28

28

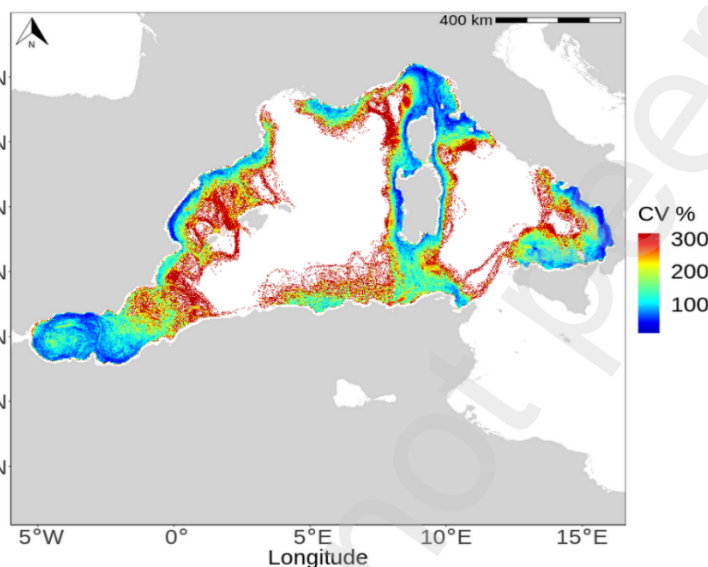
28

28

28

28

28



293

294

295

296

297

298

299

300

301

302

303

304

305

Figure 4: Density map of particles that successfully reach a recruitment zone averaged for the period 2010 to 2020, based on simulations carried out with the MedMFC model in the Western Mediterranean. The interannual variability of these trajectories is expressed by a coefficient of variation (CV).

recurrent along the study period. In contrast, other areas, such as the Balearic Islands, have less connection with the coastlines, or at least less regularly along the study period. Lastly, the Alboran Sea emerges as a significant exchange hub for larvae along its various coastlines, yet it has limited connection with the rest of the Western Mediterranean.

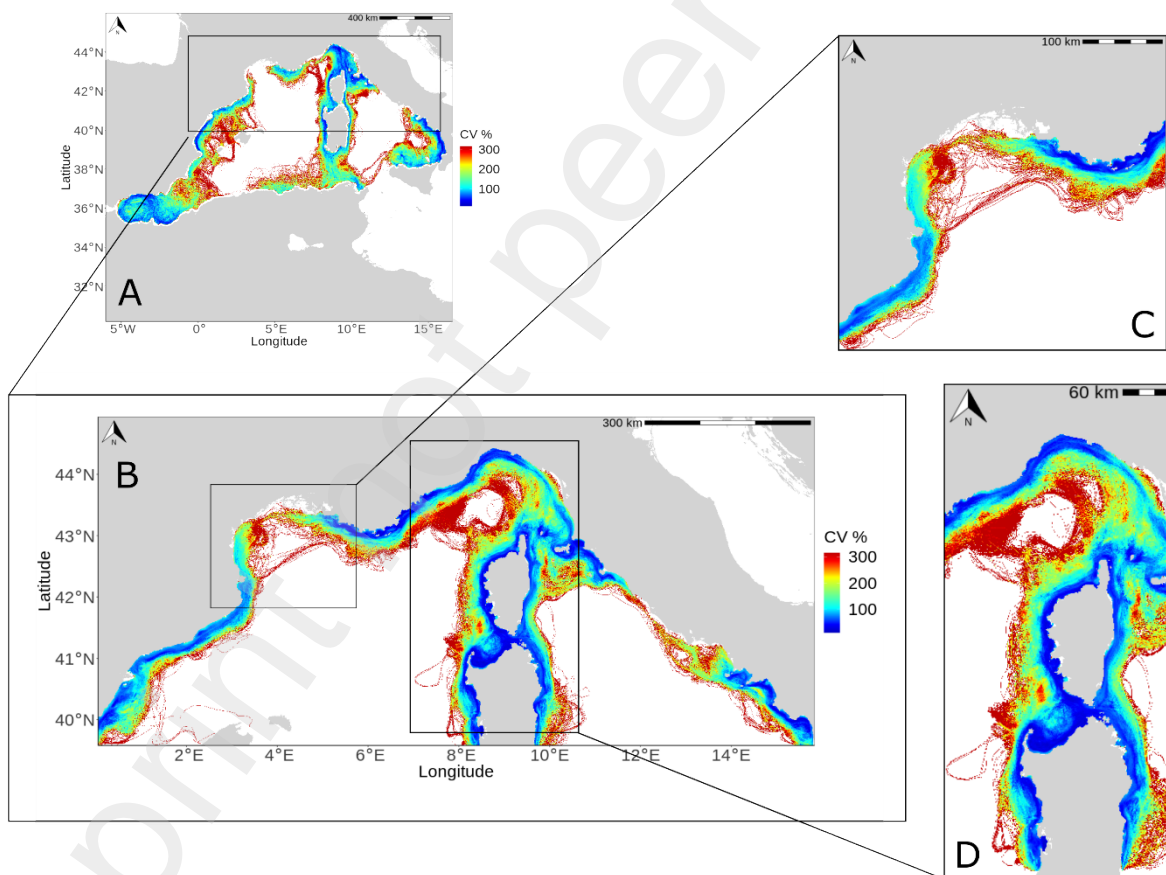
The MARS3DMed model (Fig. 5) reveals that trajectories with low coefficients of variation primarily connect nearby coastal areas, at times forming interconnected sets over the course of the eleven considered years. This is exemplified by the routes appearing on both sides along Corsica and Sardinia.

3.1 Exploring multi-scale trends over the entire temporal period (2010-2020)

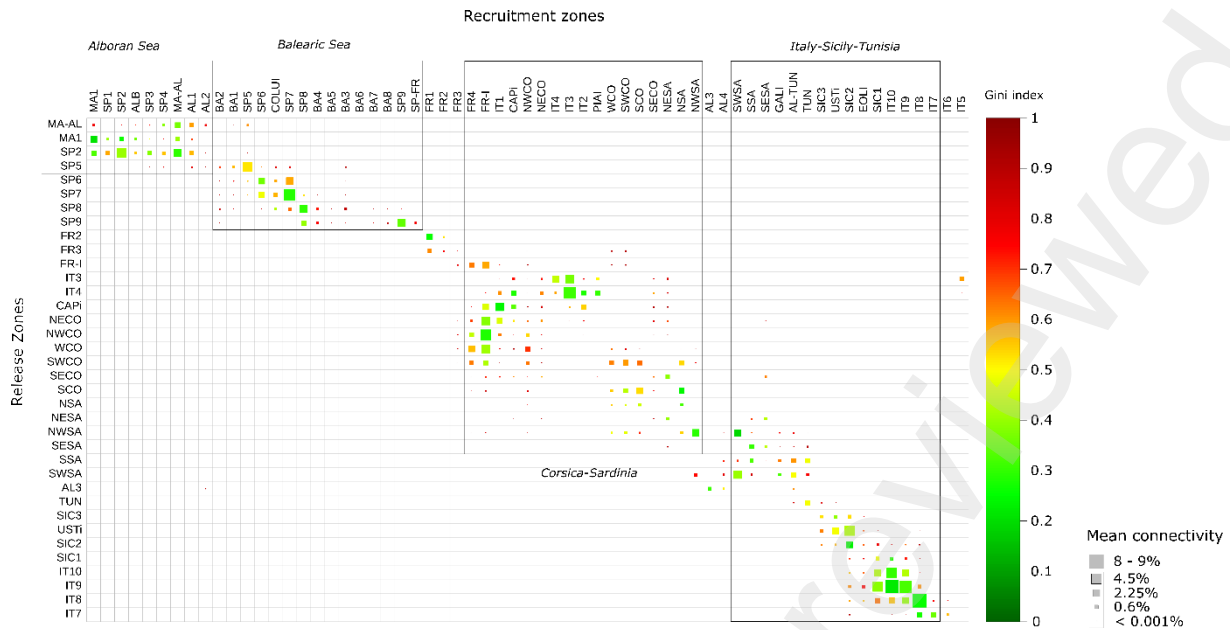
Maps of particle density's coefficient of variation (CV) computed over the entire study period and domain covered by the MedMFC model highlight the principal simulated routes and their temporal variability for larvae transported from spawning to recruitment zones (Fig. 4). We note a continuity in the simulated larval dispersal pattern of *Maja squinado* between the North and South around Corsica and Sardinia, with low CV values, indicating that this pattern is

306 The broader geographic window used with MedMFC allows for the identification of routes in the
 307 southern Western Mediterranean, particularly in the Alboran Sea, which is minimally or not connected
 308 to the rest of the sub-basins. Furthermore, the Balearic Islands are geographically isolated, although a
 309 few trajectories (with very high coefficients of variation) exhibit weak connectivity to the Spanish
 310 coastlines over the studied period. The southern coastlines of Sardinia are connected with the Tunisian
 311 coastlines on a regular basis over time. This creates a group with probable larval exchanges between
 312 Tunisia, Sardinia, and then Corsica moving northward.

313
 314 The Gulf of Lion is also a site of significant exchanges, with distinct routes emerging: one arriving from
 315 the east and another departing towards the west. Notwithstanding the high CV (panel C of Fig. 5) of
 316 these routes, they play a pivotal role in regional connectivity. In the easternmost part of the Western
 317 Mediterranean, there is also a coastal route along the Sicilian-Italian coastline with minimal connectivity
 318 to the rest of the basin, with the exception of a few trajectories (with high CV) connecting to the Tunisian
 319 coasts.



320
 321
 322 Figure 5: Trajectory densities for the entire period from 2010 to 2020 generated using two hydrodynamic models
 323 with different geographical windows and foci. A: Simulations carried out with the MedMFC model in the western
 324 Mediterranean. B: Simulations carried out with the MARS3DMed model in the north-western Mediterranean,
 325 allowing finer resolution focuses in C (Gulf of Lion) and D (Sardinia-Corsica ensemble). The variability of the
 326 trajectories over time is expressed by the coefficients of variation (CVs).
 327



328

329

330 Figure 6: The connectivity matrix was constructed on the basis of simulations conducted with the MedMFC model
 331 in the Western Mediterranean, spanning the period from 2010 to 2020. The release zones are displayed on the
 332 vertical axis, while the recruitment zones appear on the horizontal axis.

333

334 The connectivity matrix (Fig. 6) was organized in a manner consistent with the Mediterranean sub-
 335 basins. The maximum connectivity values of approximately 9% were obtained in the cluster Italy-Sicily-
 336 Tunisia, between the IT8 and IT9 zones in the southern Tyrrhenian Sea. In the Alboran Sea, we observe
 337 regular connectivity relationships (as indicated by low Gini index) and remarkably high local retention
 338 values for MA1 and SP2. In the Balearic Sea, the most notable elements are the high local retention
 339 within SP7, SP8 and SP9, all with low Gini indices. The Balearic Islands BA1 to BA9 are connected by
 340 small amount of particles and with Gini indices higher than 0.5. The Corsica-Sardinia area and the coasts
 341 of the Ligurian Sea have connections close to the maximum of obtained connectivity values (e.g., IT3
 342 with IT4, NWCO with FR-I, WCO with FR-I) with low Gini indices.

343

344 Local retention values in Corsica can reach high percentages, as for the NWCO, but with an intermediate
 345 Gini index. In the same way, we observe an intermediate level of connectivity between the Corsican and
 346 Sardinian zones. Thus, in general, we observe relatively regular exchanges between Corsica, Sardinia
 347 and the Ligurian coasts. Finally, the last remarkable group is that of the Italian, Sicilian and Tunisian
 348 coasts, where we obtain strong connectivity between zones IT7 to IT10 with strong local retention within
 349 each of these zones as well, and low Gini indices. The Tunisian zone is connected to the Sardinian ones,
 350 and the Sicilian zones are connected to both the Aeolian Islands and the Italian zones south of the
 351 Tyrrhenian Sea.

352

353

354

355 3.2 Analysis of trends in light of global change signals in the Western Mediterranean

356 3.2.1 Warming signals and comparison of larval recruitment kernels

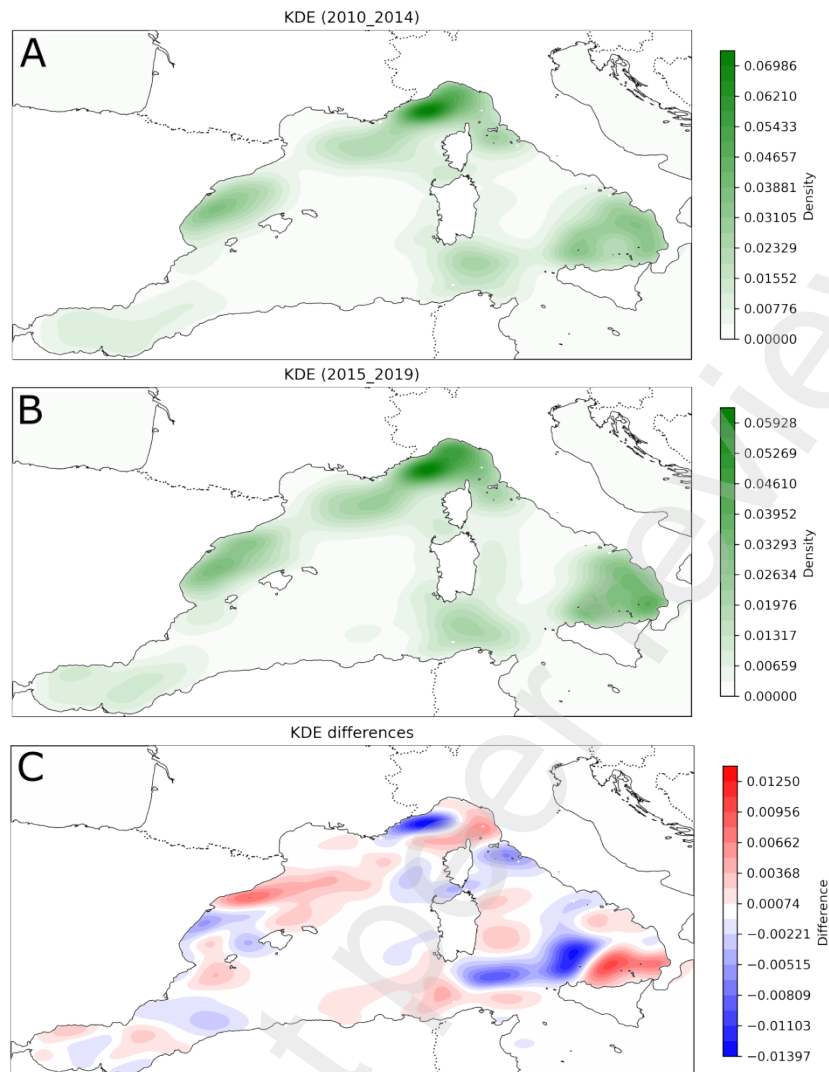
357 The kernel density estimates (KDE) map for the period 2010-2014 (Fig. 7A) shows higher maximum
358 density values than for the 2015-2019 scenario (Fig. 7B). However, the areas of highest concentration
359 remain similar, i.e., the Ligurian Sea, the southern Tyrrhenian Sea, the Balearic Sea, and to a lesser
360 extent the area between Tunisia and southern Sardinia. The map of differences between the two time
361 periods (Fig. 7C) shows areas where the density has decreased in blue, such as the northern region of
362 Italy, particularly Liguria and Tuscany, and parts of the Balearic Sea, Alboran Sea and Tyrrhenian Sea.
363 On the other hand, an increase in density is observed in the southern Tyrrhenian Sea, particularly around
364 Sicily and Tunisia, and in areas off the northwestern coast of Italy and northeastern coast of Spain.

365

366

367

368



369
370
371
372
373
374

Figure 7: Kernel density estimates (KDEs) of particle locations at the end of the PLD obtained using the MedMFC configuration for (A) 2010-2014 (B) 2015-2019 (C) shows the differences between the two time periods.

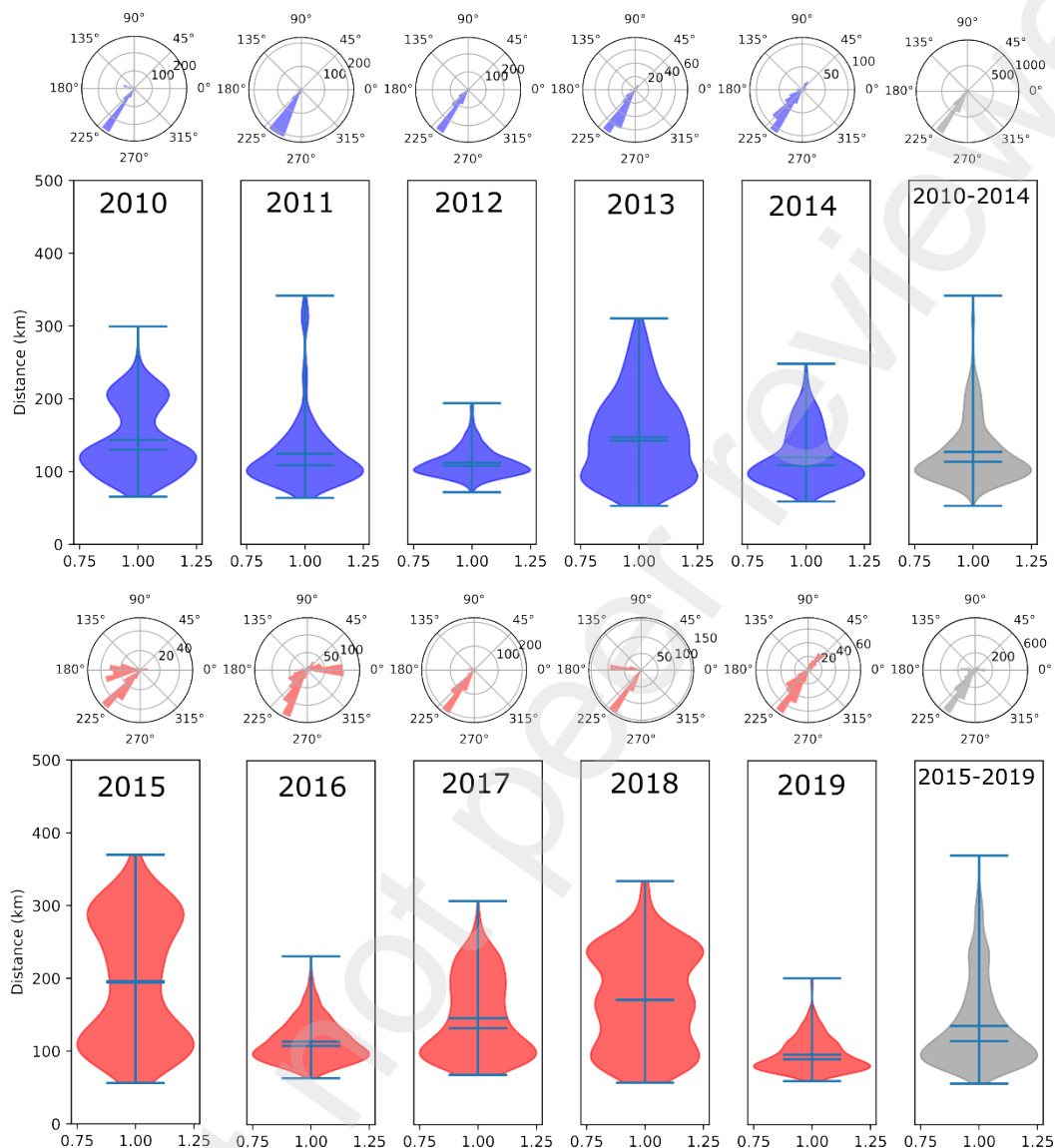
375

3.2.3 Dispersal distances and orientations in a changing Mediterranean Sea

376
377
378
379
380
381
382
383
384

The following analyses and results present two contrasting areas from the perspective of simulated connectivity and the status of *Maja squinado* in the Mediterranean. The Catalan coast (SP9; Figure 2) is the area that connects the largest number of recruitment areas in the Balearic Islands, but with low connectivity percentages and high Gini indices (Fig. 6). Furthermore, the literature and supplementary approaches have demonstrated that *M. squinado* has almost disappeared from the Balearic Islands, rendering this area a primary focus of interest. This area contrasts with the Corsica-Sardinia zones where the spinous spider crab is still exploited. Consequently, it was decided to compare it in this analysis with the southwestern Corsica zone (SWCO; Fig. 2). The latter exhibits in the matrix a number of significant connections with other zones (Fig. 6). It is also included in what appears to be a cluster of larval

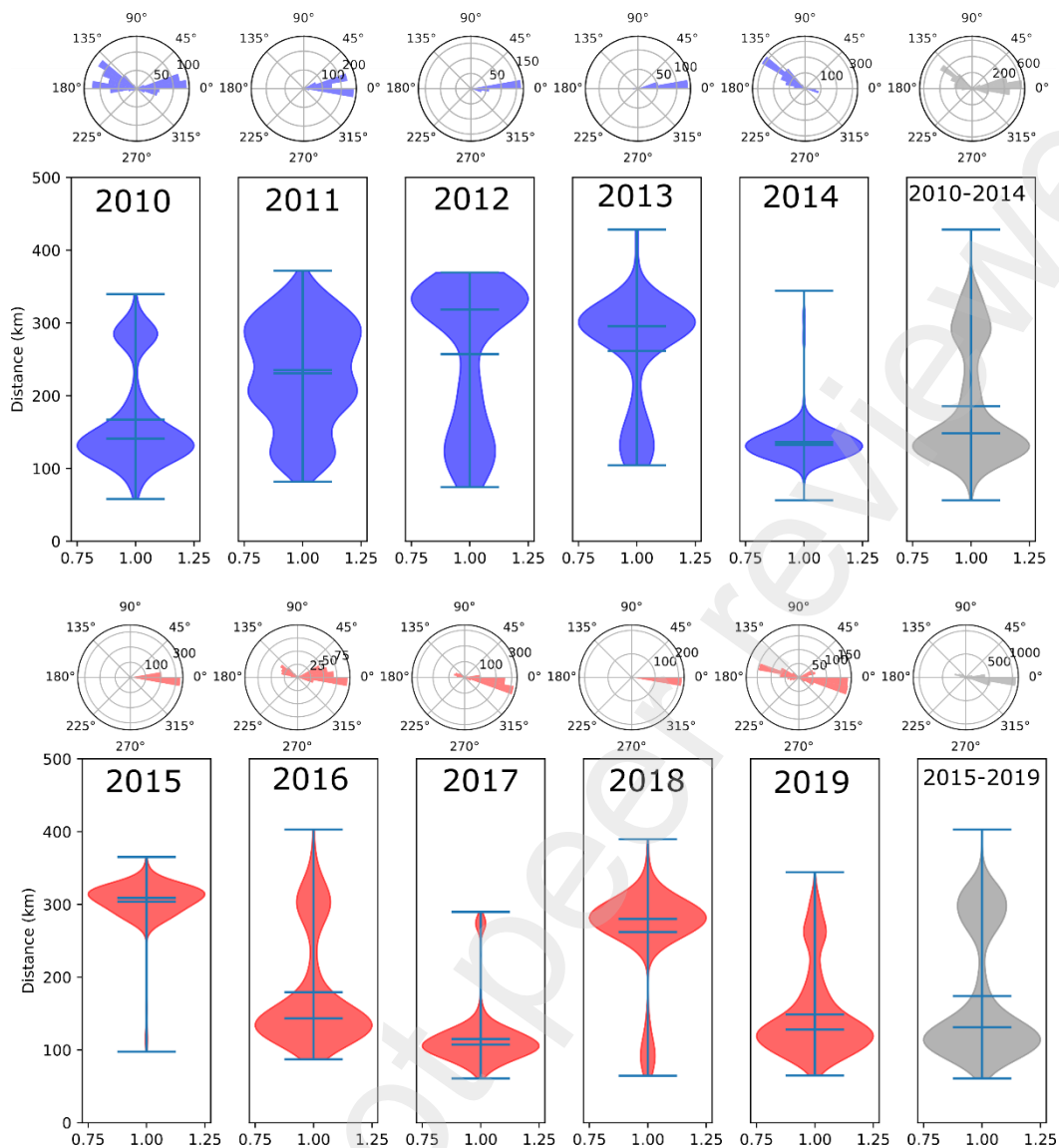
385 exchange between Tunisia, Sardinia, Corsica, and the Ligurian Sea, in connection with other areas such
 386 as those in southern Corsica (SCO and SECO in Fig. 2).
 387



388
 389
 390 Figure 8: Violin plots showing the distribution of distances traveled by larvae that have successfully reached a
 391 recruitment area from the Catalan coast release zone (SP9; Figure 2) for different time periods. Wind roses show
 392 the distribution of directions traveled by these larvae.
 393

394 The mean distance travelled by larvae from SP9 exhibited a slight increase from 127.06 km (2010-2014)
 395 to 135.60 km (2015-2019). Furthermore, the standard deviation of the distance increased from 44.35 km
 396 to 58.82 km, indicating greater variability in the distances travelled. The standard deviation of the
 397 direction of travel also increased, from 57.59° to 83.01°, indicating greater variability in the dispersal
 398 directions. Indeed, the distribution of directions was bimodal in 2015, 2016, 2018, and 2019, as opposed
 399 to being unimodal in all years from 2010 to 2014 (Fig. 8).

400



401
402

403 Figure 9: Violin plots showing the distribution of distances traveled by larvae that have successfully reached a
404 recruitment area from the Southwestern Corsican zone (SWCO; Figure 2) for different time periods. Wind roses
405 show the distribution of directions traveled by these larvae.

406

407 The mean distance travelled by larvae was found to be slightly shorter in the 2015-2019 period (174.07
408 km) compared to the 2010-2014 period (185.60 km), according to data from SWCO. However, the
409 variability in distances travelled in the 2015-2019 period was greater than in the 2010-2014 period
410 (standard deviation 85.23 km and 77.93 km, respectively). The mean direction of movement exhibited
411 a notable shift, from 58.51° to 1.10°, and the variability of directions also increased during the 2015-
412 2019 period. Indeed, the mean direction of dispersal averaged over the 2010-2014 period exhibited two
413 peaks, at approximately 135° and 0°, respectively. In contrast, only the 0° peak was observed from 2015
414 to 2019 (Fig. 9).

415
416
417
418

419 4. Discussion

420 The simulations generated by the MARS3DMed model are intended to reinforce and refine the findings
421 observed in the MedMFC model simulations. This was made possible by meticulously delineating
422 specific coastal exchanges, which could only be discerned with a higher level of detail. Consequently,
423 the simulations are more closely aligned with field reality in the MARS3DMed model than in MedMFC,
424 despite the broader geographic scope being essential to encompass pertinent release and recruitment
425 sites. It is crucial to acknowledge that a model with a higher resolution will yield results that are more
426 reflective of reality than a model with a less precise resolution. This is because the latter is prone to
427 underestimating particle dispersion (Saint-Amand et al., 2023).

428

429 The results of simulations conducted in the Western Mediterranean have demonstrated, for the first time
430 with a biophysical modelling approach at this spatiotemporal scale, that *Maja squinado*, with its
431 relatively short PLD, exhibits limited dispersal capabilities. In general, the dispersion paths taken by the
432 organism exhibit minimal variation over time, both in terms of distance and direction. These paths align
433 with the predominant current patterns of the region and can be dispersed to distances exceeding eight
434 times the average observed distance. Medium-scale oceanographic features, such as fronts and eddies,
435 have been identified as key mechanisms affecting dispersion in these specific areas (Alcaraz et al.,
436 2007). Although vertical migration is commonly accepted in crustaceans of the Brachyurans group, its
437 effects were not tested in this study and were parameterised as active in our simulations. However, in
438 other species, this migration has been demonstrated in the literature to constrain the distance and speed
439 of dispersion (Zakardjian et al., 1999). As with other Brachyurans, larval dispersion and migration may
440 be defined here by the dominant current patterns of the location (Anger et al., 2015), as well as the
441 presence or absence of suitable habitats for spawning and recruitment.

442

443 In the presented study, observations were made in the context of the warming of surface waters in the
444 Mediterranean, with particular attention paid to the acceleration observed between 2014 and 2015
445 (Margirier et al., 2020; Pastor et al., 2020). The graphical observations indicate differences between the
446 two scenarios in the Mediterranean for the two subsampled areas, SP9 and SWCO. While statistical
447 analysis would have been relevant, the limited quantity of data and the low number of trajectories,
448 combined with their irregularity, did not permit a statistically robust analysis. A recommendation for
449 future studies attempting to hypothesise about the synergy of causes of changes in dispersal dynamics,
450 involving global change, would be to collect more data to improve the robustness of the analyses,
451 particularly for areas where the number of observations is currently limited, such as the Balearic Islands
452 and their connectivity with the closest coastlines, where reports of *M. squinado* are still made (the
453 Spanish coasts, for example, notably SP9). Consequently, although statistical analysis is constrained by
454 the quantity and variability of the data, the graphical observations indicate potential changes in the

455 dispersal behaviours of *Maja squinado* larvae in response to global warming. This finding warrants
456 further investigations and increased attention to these dynamics. The KDE results reinforce the
457 hypothesis that the acceleration of global warming, in particular the increase in the temperature of
458 surface waters, could affect the dispersal trajectories of *Maja squinado* larvae predicted by the
459 simulations. The observed changes in particle densities indicate that traditionally favourable areas may
460 become less conducive to larval concentration, while other areas may see an increase in density. These
461 kinds of observations, when considered in conjunction with the population dynamics of an exploited
462 species with an IUCN status of non-evaluated, could prove crucial for the development of future
463 management measures. Another crucial link to be considered between global change and larval
464 dispersion dynamics in *Maja squinado* is the biological model itself. Indeed, temperature could be a
465 significant factor conditioning spawning schedules, thus affecting the quality and quantity of eggs laid.
466 For example, studies have demonstrated the effects of ovarian mutations in the freshwater shrimp
467 (*Penaeus merguensis*, Hoang et al., 2002), and a meta-analysis has highlighted the impact of
468 temperature on various stages in brachyuran crabs, indicating that spawning is advanced as temperatures
469 rise (Azra et al., 2019). Furthermore, another study indicates a correlation between temperature
470 evolution and crab population dynamics. This study demonstrates that environmental temperature
471 variations correlate with the spatial and temporal variation of the crab *Portunus armatus* during the
472 breeding period (Johnson and Yeoh, 2021). To date, no study has specifically focused on *Maja squinado*
473 in the Western Mediterranean and examined the evolution of its thermal tolerances and spawning
474 schedule in light of global change and surface water warming. Nevertheless, it would be beneficial to
475 observe the results of forthcoming studies with a view to enhancing the calibration of models that could
476 shed light on the dynamics of its populations in a changing Mediterranean.

477

478 It is therefore inaccurate to draw a direct cause-and-effect relationship between global change and
479 changes in larval dispersal and connectivity in species with a biphasic life cycle. Therefore, we prefer
480 to discuss the interaction of environmental and biological traits parameters as a "synergy". Nevertheless,
481 since current patterns are the primary driver of larval dispersion in larvae incapable of swimming, there
482 is a correlation between minor or major changes in current regimes and global changes, which in turn
483 result in cascading effects on zooplankton species and their dispersion. Further in-depth studies are
484 warranted. Indeed, a number of factors have been identified as being of crucial importance for the
485 survival and dispersion of crustacean larvae, including seasonal variations in currents, water
486 temperature, and the availability of food resources. These factors have been demonstrated to be of
487 importance in a number of studies, including those by Anger (1991), Bryars & Havenhand (2006), and
488 Epifanio & Garvine (2001b). In the absence of warming scenarios, our findings indicate that interannual
489 variability in connectivity between sites is the most significant factor. This may be attributed to the
490 impact of current global warming on surface temperatures and, consequently, on currents on an annual
491 basis. A more detailed analysis of these parameters and their implementation in future models could

492 provide a better understanding of the observed dispersion patterns, while explaining the contribution of
493 water warming to the interannual variability (Corrochano-Fraile et al., 2022; Šargač et al., 2022).

494

495 The findings of this study enable the prediction of large-scale and long-term trends in *Maja squinado*, a
496 species whose ecology and population dynamics remain poorly understood. Along the coasts where
497 areas favorable to the spawning of the spinous spider crab have been parameterized, connectivity over
498 multiple sites can occur between relatively distant locations through various intermediaries. It is likely
499 that these coastal zones exhibit small-scale circulation dynamics that trap larvae near the release site,
500 influenced by interactions with eddies and seafloor topography. Sites with high local retention can
501 maintain significant local recruitment, supporting a population over time and reducing the risk of larval
502 loss or recruitment failure due to phenotype-environment mismatches (King et al., 2023). Based on the
503 selected release sites, larval exchanges in the Mediterranean appear to be confined within distinct basins.
504 For instance, there is a scarcity of larval exchanges between the Algero-Provençal basin and the
505 Tyrrhenian Sea via the Ligurian Sea. Similarly, the Alboran Sea and the Balearic Islands appear isolated
506 from the rest of the coastlines. With the exception of the Northwestern Mediterranean, where
507 connectivity between Corsica, Italy, and the French coastlines is consistent and regular over the study
508 period, it is challenging to estimate links between more distant sites due to the relatively short larval
509 duration of the spider crab. There is almost no observable connection between Catalonia and the Balearic
510 Islands, suggesting low connectivity with these islands. This isolation can be attributed to the
511 hydrodynamically complex nature of the Balearic Sea, resulting from interactions between different
512 water masses and the island's topography, which limits species exchange between these areas and other
513 regions (López-Jurado et al., 1995; Pinot et al., 2002). This research contributes to our understanding of
514 the exploitation and preservation challenges of *M. squinado* in the Mediterranean by offering initial
515 observations on connectivity and population dynamics, highlighting the constraints on larval exchanges
516 within the Mediterranean's distinct basins.

517

518 The reliability and significance of predictions derived from biophysical models are becoming
519 increasingly evident when compared to alternative scientific methodologies. Consequently, it can be
520 postulated that population genetic studies on *M. squinado* may offer invaluable insights that could
521 facilitate more accurate parameterisation of future simulations. For instance, they could provide further
522 understanding of the species' dispersal patterns by identifying specific sub-populations around these
523 islands and on a broader scale. Nevertheless, the findings of these studies elucidate the behaviour of
524 *Maja squinado* larvae and the potential for dispersion from a known population location. This study
525 focuses on larval dispersion, and it is important to note that several factors affect larval recruitment,
526 including predation, competition, and ontogenetic traits (Anger et al., 2015). For instance, some species
527 may benefit from the presence of larvae as food, while others may act as potential predators (Anger et
528 al., 2015; Torres et al., 2013). The present model does not include the factors affecting larval mortality,

529 which are influenced by interspecific relationships. Future simulations could therefore benefit from
530 further studies in order to refine the parameters. For example, it would be beneficial to be able to specify
531 the quality and quantity of spawning, as well as the factors influencing the survival of larval flows from
532 one year to the next.

533

534 It is evident that the results of the study largely depend on the ability to identify source and sink sites
535 within the dispersion system. For the purposes of management, the dispersion characteristics of sites
536 can be considered in order to assess their importance in a small-scale system. Sites that release more
537 larvae than they retain may be vulnerable to population collapse due to fishing, resulting in a decrease
538 in the number of potentially recruitable larvae at another site (Cowen et al., 2002; Steneck et al., 2006).
539 This may be particularly pertinent to the Balearic Islands, which have limited larval recruitment from
540 Spain and possibly the Maghreb, while also being subject to overfishing (Garcia, 2007). The prevalence
541 of short-distance dispersal, in comparison to other species that pose invasion concerns, raises questions
542 about the role of islands in large-scale species dispersal.

543

544 Areas with high connectivity, such as the Corsican and Sardinian coastlines, along with Sicily, Tunisia,
545 and southern Sardinia, could be the subject of studies on the benefits of establishing a network of
546 protected areas. This would favor and protect the exchange of larvae and the pools of breeding
547 individuals. Such measures could help to prevent scenarios where potentially overly isolated areas cut
548 off from exchanges have experienced population collapses and consequently the cessation of fishing
549 activities, as seen in the Balearic Islands due to depleted stocks. These results could be supported by
550 genetic and phylogenetic studies, which would show genetic differentiation or proximity between
551 different areas, indicating the existence of several sub-populations. Such studies have been conducted
552 on the sister species *Maja brachydactyla* in the Atlantic, which have highlighted the importance of the
553 Strait of Gibraltar in defining species boundaries (Abello et al., 2014). Identifying genetic barriers and
554 gene flows would be useful indicators for assessing dispersion and differentiation between populations
555 (Gilg & Hilbish, 2003). This information is crucial for establishing protected areas for the species and
556 identifying nursery zones.

557

558 **5. Conclusion**

559 This study represents the first larval dispersal model of *Maja squinado* on a Western Mediterranean
560 scale. Our analyses, combining graphical observations, have provided insights into the dispersal patterns
561 and potential impacts of climate change on the larval stages of this commercially exploited species. The
562 relatively short pelagic larval duration (PLD) of *Maja squinado* likely explains the observed relationship
563 between the disappearance of the species in heavily fished areas and poorly connected zones. For
564 example, the Balearic Islands, which are geographically isolated, do not consistently connect with other

565 coastal areas due to the limited pelagic larval duration of the spinous spider crab. This isolation could
566 be a primary factor in the species' decline in these regions. However, this hypothesis requires further
567 investigation, including genetic analyses, to better understand the level of population isolation. The
568 predictions from our simulations allow us to observe interannual changes, especially in the context of
569 post-warming acceleration shifts. It is of the utmost importance to incorporate these climatic
570 considerations into future models, as global changes not only affect the dynamics of ocean currents,
571 which are crucial for larval dispersal, but also directly impact the physiology of the modelled organisms.
572 Our results emphasise the necessity to integrate biophysical modelling approaches with other
573 methodologies, particularly genetic studies. For instance, it is of the utmost importance to determine
574 whether the populations within the Sardinia-Corsica cluster are homogeneous or exhibit significant
575 genetic differentiation. Such combined approaches will provide a more comprehensive understanding
576 of the population dynamics and connectivity of *Maja squinado*. In conclusion, while the current study
577 provides valuable insights, it also highlights the necessity for multidisciplinary research to address the
578 complex interactions between environmental changes, species physiology, and population connectivity.
579

580 6. References

- 581 Abelló, P., Guerao, G., Salmerón, F., & Raso, J. E. G. (2014). *Maja brachydactyla* (Brachyura: Majidae)
582 in the western Mediterranean. *Marine Biodiversity Records*, 7, e77.
- 583 Adams, D. K., Arellano, S. M., & Govenar, B. (2012). Larval dispersal: vent life in the water column.
584 *Oceanography*, 25(1), 256-268.
- 585 Alcaraz, M., Calbet, A., Estrada, M., Marrasé, C., Saiz, E., & Trepát, I. (2007). Physical control of
586 zooplankton communities in the Catalan Sea. *Progress in Oceanography*, 74(2-3), 294-312.
- 587 Al-Qattan, N., Herbert, G. S., Spero, H. J., McCarthy, S., McGeedy, R., Tao, R., & Power, A. M. (2023).
588 A stable isotope sclerochronology-based forensic method for reconstructing debris drift paths with
589 application to the MH370 crash. *AGU Advances*, 4(4), e2023AV000915.
- 590 Angeletti, R., Binato, G., Guidotti, M., Morelli, S., Pastorelli, A. A., Sagratella, E., ... & Stacchini, P.
591 (2014). Cadmium bioaccumulation in Mediterranean spider crab (*Maja squinado*): Human consumption
592 and health implications for exposure in Italian population. *Chemosphere*, 100, 83-88.
- 593 Anger, K. (1991). Effects of temperature and salinity on the larval development of the Chinese mitten
594 crab *Eriocheir sinensis* (Decapoda: Grapsidae). *Marine ecology progress series. Oldendorf*, 72(1), 103-
595 110.
- 596 Anger, K., Queiroga, H., & Calado, R. (2015). Larval development and behaviour strategies in
597 Brachyura. In *Treatise on Zoology-Anatomy, Taxonomy, Biology. The Crustacea, Volume 9 Part C (2*
598 *vols)* (pp. 317-374). Brill.
- 599 Arakawa, A. (1977). Computational design of the basic dynamical processes of the UCLA general
600 circulation model. *Methods in Computational Physics. Advances in Research and Application, Vol. 17:*
601 *General circulation models of the atmosphere*, 337.

- 602 Azra, M. N., Chen, J. C., Hsu, T. H., Ikhwanuddin, M., & Abol-Munafi, A. B. (2019). Growth, molting
603 duration and carapace hardness of blue swimming crab, *Portunus pelagicus*, instars at different water
604 temperatures. *Aquaculture reports*, 15, 100226.
- 605 Balss, H., Crustacea VII: Decapoda Brachyura (Oxyrhyncha und Brachyrhyncha) und geographische
606 Übersicht über Crustacea Decapoda. Beitr. Kennt. Meeresfauna Westafr., 3 (1922) 71–110.
- 607 Begon, M., Owensend, C., Harper, J. (2005). Ecology: from Individuals to Ecosystems. In *Freshwater
608 Biology—FRESHWATER BIOL* (Vol. 51).
- 609 Bianchi, C. N., & Morri, C. (2000). Marine biodiversity of the Mediterranean Sea: situation, problems
610 and prospects for future research. *Marine pollution bulletin*, 40(5), 367-376.
- 611 Bousquet, C., Bouet, M., Patrissi, M., Cesari, F., Lanfranchi, J. B., Susini, S., ... & Durieux, E. D. (2022).
612 Assessment of catch composition, production and fishing effort of small-scale fisheries: The case study
613 of Corsica Island (Mediterranean Sea). *Ocean & Coastal Management*, 218, 105998.
- 614 Bryars, S. R., & Havenhand, J. N. (2006). Effects of constant and varying temperatures on the
615 development of blue swimmer crab (*Portunus pelagicus*) larvae: Laboratory observations and field
616 predictions for temperate coastal waters. *Journal of Experimental Marine Biology and Ecology*, 329(2),
617 218-229.
- 618 Calado, R., Guerao, G., Gras, N., Cleary, D. F., & Rotllant, G. (2013). Contrasting habitats occupied by
619 sibling spider crabs *Maja squinado* and *Maja brachydactyla* (Brachyura, Majidae) can influence the
620 biochemical variability displayed by newly hatched larvae. *Journal of plankton research*, 35(3), 684-
621 688.
- 622 Carlson, A., Maynou, F., Basurco, B., & Bernal, M. (2016). Chapitre 2-Gestion des ressources marines
623 vivantes. In *Méditerranée 2016 : Zéro gaspillage en Méditerranée* (pp. 51-70). Presses de Sciences Po. Coll
624 et al., 2014.
- 625 Corrochano-Fraile, A., Adams, T. P., Aleynik, D., Bekaert, M., & Carboni, S. (2022). Predictive
626 biophysical models of bivalve larvae dispersal in Scotland. *Frontiers in Marine Science*, 9, 985748.
- 627 Cowen, R. K. (2002). Larval Dispersal and Retention and Consequences for. *Coral reef fishes: dynamics
628 and diversity in a complex ecosystem*, 149.
- 629 Cowen, R. K., Gawarkiewicz, G., Pineda, J., Thorrold, S., & Werner, F. (2002, November). Population
630 connectivity in marine systems. In *Report of a workshop to develop science recommendations for the
631 National Science Foundation* (Vol. 84, pp. 119-119).
- 632 de Mello, C., Barreiro, M., Hernandez-Garcia, E., Trinchin, R., & Manta, G. (2023). A Lagrangian study
633 of summer upwelling along the Uruguayan coast. *Continental Shelf Research*, 258, 104987.
- 634 Durán, J., Palmer, M., & Pastor, E. (2013). Growing reared spider crabs (*Maja squinado*) to sexual
635 maturity: the first empirical data and a predictive growth model. *Aquaculture*, 408, 78-87.
- 636 Durán, J., Pastor, E., Grau, A., & Valencia, J. M. (2012). First results of embryonic development,
637 spawning and larval rearing of the Mediterranean spider crab *Maja squinado* (Herbst) under laboratory
638 conditions, a candidate species for a restocking program. *Aquaculture Research*, 43(12), 1777-1786.
- 639 Epifanio, C. E., & Garvine, R. W. (2001a). Larval Transport on the Atlantic Continental Shelf of North
640 America: A Review. *Estuarine, Coastal and Shelf Science*, 52, 51-77.
641 <https://doi.org/10.1006/ecss.2000.0727>.
- 642 Escudier, R., Clementi, E., Cipollone, A., Pistoia, J., Drudi, M., Grandi, A., Lyubartsev, V., Lecci, R.,
643 Aydogdu, A., Delrosso, D., Omar, M., Masina, S., Coppini, G., & Pinardi, N. (2021). A High Resolution

- 644 Reanalysis for the Mediterranean Sea. *Frontiers in Earth Science*, 9.
645 <https://www.frontiersin.org/articles/10.3389/feart.2021.702285>.
- 646 FAO. (2020). *La situation mondiale des pêches et de l'aquaculture 2020 : La durabilité en action*. FAO.
647 <https://doi.org/10.4060/ca9229fr>.
- 648 Flores-Valiente, J., Lett, C., Colas, F., Pecquerie, L., Aguirre-Velarde, A., Rioual, F., ... & Brochier, T.
649 (2023). Influence of combined temperature and food availability on Peruvian anchovy (*Engraulis*
650 *ringens*) early life stages in the northern Humboldt Current system: A modelling approach. *Progress in*
651 *Oceanography*, 215, 103034.
- 652 Garcia, L. (2007). *Garcia Ll (2007) Els crançs de les Balears. Quaderns de Natura de les Balears. Ed*
653 *Documenta Balear SL, Palma de Mallorca, 104 pp.*
- 654 Gary, S. F., Fox, A. D., Biastoch, A., Roberts, J. M., & Cunningham, S. A. (2020). Larval behaviour,
655 dispersal and population connectivity in the deep sea. *Scientific Reports*, 10(1), Article 1.
656 <https://doi.org/10.1038/s41598-020-67503-7>.
- 657 Gilg, M. R., Hilbish, J. (2003). The Geography of marine larval dispersal: coupling genetics with fine-
658 scale physical oceanography. *Ecology*, 84(11), 2989-2998. <https://doi.org/10.1890/02-0498>.
- 659 Gualtieri, J.-S., Aiello, A., Antoine-Santoni, T., Poggi, B., & DeGentili, E. (2013). Active tracing of
660 *Maja squinado* in the Mediterranean Sea with wireless acoustic sensors: Method, results and
661 perspectives. *Sensors (Basel, Switzerland)*, 13(11), 15682-15691. <https://doi.org/10.3390/s131115682>.
- 662 Guerao, G., & Rotllant, G. (2010). Development and growth of the early juveniles of the spider crab
663 *Maja squinado* (Brachyura: Majoidea) in an individual culture system. *Aquaculture*, 307(1-2), 105-110.
- 664 Guerao, G., Rotllant, G., Gisbert, E., Uyà, M., & Cardona, L. (2016). Consistent habitat segregation
665 between sexes in the spider crabs *Maja brachydactyla* and *Maja squinado* (Brachyura), as revealed by
666 stable isotopes. *Scientia Marina*, 80. <https://doi.org/10.3989/scimar.04236.23B>.
- 667 Herbst, J.F.W., 1788. Versuch einer Naturgeschichte der Krabben und Krebse nebst einer
668 systematischen Beschreibung ihrer verschiedene-nen Arten. Lange, G.A., Berlin and Stralsund, pp. 207–
669 238.
- 670 Hixon, M. A., & Jones, G. P. (2005). Competition, Predation, and Density-Dependent Mortality in
671 Demersal Marine Fishes. *Ecology*, 86(11), 2847-2859. <https://doi.org/10.1890/04-1455>.
- 672 Hoang, T., Lee, S. Y., Keenan, C. P., & Marsden, G. E. (2002). Effect of temperature on spawning of
673 *Penaeus merguensis*. *Journal of Thermal Biology*, 27(5), 433-437.
- 674 Imzilen, T., Kaplan, D. M., Barrier, N., & Lett, C. (2023). Simulations of drifting fish aggregating device
675 (dFAD) trajectories in the Atlantic and Indian Oceans. *Fisheries Research*, 264, 106711.
676 <https://doi.org/10.1016/j.fishres.2023.106711>.
- 677 Jahnke, M., & Jonsson, P. R. (2022). Biophysical models of dispersal contribute to seascape genetic
678 analyses. *Philosophical Transactions of the Royal Society B: Biological Sciences*, 377(1846), 20210024.
679 <https://doi.org/10.1098/rstb.2021.0024>.
- 680 Johnston, D. J., & Yeoh, D. E. (2021). Temperature drives spatial and temporal variation in the
681 reproductive biology of the blue swimmer crab *Portunus armatus* A. Milne-Edwards, 1861 (Decapoda:
682 Brachyura: Portunidae). *Journal of Crustacean Biology*, 41(3), ruab032.
- 683 King, S., Saint-Amand, A., Walker, B. K., Hanert, E., & Figueiredo, J. (2023). Larval dispersal patterns
684 and connectivity of *Acropora* on lorida's Coral Reef and its implications for restoration. *Frontiers in*
685 *Marine Science*, 9. <https://www.frontiersin.org/articles/10.3389/fmars.2022.1038463>.

- 686 Lazure, P., & Dumas, F. (2008). An external–internal mode coupling for a 3D hydrodynamical model
687 for applications at regional scale (MARS). *Advances in Water Resources*, 31(2), 233-250.
688 <https://doi.org/10.1016/j.advwatres.2007.06.010>.
- 689 Lett, C., Ayata, S.-D., Huret, M., & Irisson, J.-O. (2010). Biophysical modelling to investigate the effects
690 of climate change on marine population dispersal and connectivity. *Progress In Oceanography*, 87,
691 106-113. <https://doi.org/10.1016/j.pocean.2010.09.005>.
- 692 Lett, C., Verley, P., Mullon, C., Parada, C., Brochier, T., Penven, P., & Blanke, B. (2008). A Lagrangian
693 tool for modelling ichthyoplankton dynamics. *Environmental Modelling and Software*, 23(9), 1210.
694 <https://doi.org/10.1016/j.envsoft.2008.02.005>.
- 695 López-Jurado, J. L., García-Lafuente, J. M., & Cano-Lucaya, N. (1995). Hydrographic conditions of the
696 Ibiza Channel during November 1990, March 1991 and July 1992.
697 <https://digital.csic.es/handle/10261/317533>.
- 698 Marengo, M., Pere, A., Marchand, B., Lejeune, P., & Durieux, E. (2016). Catch variation and
699 demographic structure of common dentex (Sparidae) exploited by Mediterranean artisanal fisheries.
700 *Bulletin of Marine Science*, 92. <https://doi.org/10.5343/bms.2015.1041>.
- 701 Marengo, M., Vanalderweireldt, L., Horri, K., Patrissi, M., Santoni, M.-C., Lejeune, P., & Durieux, E.
702 (2023). Combining indicator trends to evaluate a typical Mediterranean small-scale fishery: a case study
703 of Corsica. *Regional Studies in Marine Science*, 65, 103087.
704 <https://doi.org/10.1016/j.rsma.2023.103087>.
- 705 Margirier, F., Testor, P., Heslop, E., Mallil, K., Bosse, A., Houpert, L., ... & Taillandier, V. (2020).
706 Abrupt warming and salinification of intermediate waters interplays with decline of deep convection in
707 the Northwestern Mediterranean Sea. *Scientific Reports*, 10(1), 20923.
- 708 Martín, P., Maynou, F., Stelzenmüller, V., & Sacanell, M. (2012). A small-scale fishery near a rocky
709 littoral marine reserve in the northwestern Mediterranean (Medes Islands) after two decades of fishing
710 prohibition. *Scientia Marina*, 76. <https://doi.org/10.3989/scimar.03471.07F>.
- 711 Millot, C., & Taupier-Letage, I. (2005). Circulation in the Mediterranean Sea. In A. Saliot (Éd.), *The*
712 *Mediterranean Sea* (p. 29-66). Springer. <https://doi.org/10.1007/b107143>.
- 713 Modena, M., Mori, M., & Vacchi, M. (2001). Note su alcuni crostacei malacostraci raccolti in aree
714 adiacenti alla M/C Haven (Mar Ligure). *Biologia Marina Mediterranea*, 8, 675-679.
- 715 Mura, M., & Corda, S. (2011). Crustacea Decapoda in the Sardinian Channel: a checklist. *Crustaceana*,
716 84(5-6), 667-687.
- 717 Neumann V., (1998). A review of the *Maja squinado* (Crustacea: Decapoda: Brachyura) species-
718 complex with a key to the eastern Atlantic and Mediterranean species of the genus. *Journal of Natural*
719 *History*, 32(10-11), 1667-1684. <https://doi.org/10.1080/00222939800771191>.
- 720 Okubo, A. (1994). The role of diffusion and related physical processes in dispersal and recruitment of
721 marine populations. In *The Bio-Physics of Marine Larval Dispersal* (p. 5-32). American Geophysical
722 Union (AGU). <https://doi.org/10.1029/CE045p0005>.
- 723 Ospina-Alvarez, A., Weidberg, N., Aiken, C., & Navarrete, S. (2018). Larval transport in the upwelling
724 ecosystem of central Chile: the effects of vertical migration, developmental time and coastal topography
725 on recruitment. *Progress In Oceanography*, 168. <https://doi.org/10.1016/j.pocean.2018.09.016>.
- 726 Pastor, F., Valiente, J. A., & Khodayar, S. (2020). A warming Mediterranean: 38 years of increasing sea
727 surface temperature. *Remote sensing*, 12(17), 2687.

- 728 Peliz, A., Marchesiello, P., Dubert, J., Marta-Almeida, M., Roy, C., & Queiroga, H. (2007). A study of
729 crab larvae dispersal on the eastern Iberian Shelf: Physical processes. *Journal of Marine Systems*, 68(1),
730 215-236. <https://doi.org/10.1016/j.jmarsys.2006.11.007>.
- 731 Pinardi, N., Zavatarelli, M., Adani, M., Coppini, G., Fratianni, C., Oddo, P., ... & Bonaduce, A. (2015).
732 Mediterranean Sea large-scale low-frequency ocean variability and water mass formation rates from
733 1987 to 2007: A retrospective analysis. *Progress in Oceanography*, 132, 318-332.
- 734 Pineda, J., Hare, J., & Sponaugle, S. (2007). Larval Transport and Dispersal in the Coastal Ocean and
735 Consequences for Population Connectivity. *Oceanography*, 20(3), 22-39.
736 <https://doi.org/10.5670/oceanog.2007.27>.
- 737 Pinot, J.-M., López-Jurado, J., & Riera, M. (2002). The CANALES experiment (1996-1998).
738 Interannual, seasonal, and mesoscale variability of the circulation in the Balearic Channels. *Progress In*
739 *Oceanography*, 55, 335-370. [https://doi.org/10.1016/S0079-6611\(02\)00139-8](https://doi.org/10.1016/S0079-6611(02)00139-8).
- 740 Pipitone, C., & Arculeo, M. (2003). The marine Crustacea Decapoda of Sicily (central Mediterranean
741 Sea): a checklist with remarks on their distribution. *Italian Journal of Zoology*, 70(1), 69-78.
- 742 Power, J. (1984). *Advection, Diffusion, and Drift Migrations of Larval Fish* (p. 27-37).
743 https://doi.org/10.1007/978-1-4613-2763-9_2.
- 744 Power, J. H. (1984). Advection, diffusion, and drift migrations of larval fish. In *Mechanisms of*
745 *Migration in Fishes* (pp. 27-37). Boston, MA: Springer US.
- 746 Rojas-Araos, F., Rojas-Hernández, N., Cornejo-Guzmán, S., Ernst, B., Dewitte, B., Parada, C., & Veliz,
747 D. (2024). Population genomic and biophysical modeling show different patterns of population
748 connectivity in the spiny lobster *Jasus frontalis* inhabiting oceanic islands. *Marine Environmental*
749 *Research*, 193, 106253.
- 750 Rotllant, G., Aguzzi, J., Sarria, D., Gisbert, E., Sbragaglia, V., Río, J. D., Simeó, C. G., Mánuel, A.,
751 Molino, E., Costa, C., & Sardà, F. (2015). Pilot acoustic tracking study on adult spiny lobsters (*Palinurus*
752 *mauritanicus*) and spider crabs (*Maja squinado*) within an artificial reef. *Hydrobiologia*, 742(1), 27-38.
753 <https://doi.org/10.1007/s10750-014-1959-5>.
- 754 Rotllant, G., Guerao, G., Gras, N., & Estevez, A. (2014). Larval growth and biochemical composition
755 of the protected Mediterranean spider crab *Maja squinado* (Brachyura, Majidae). *Aquatic Biology*, 20,
756 13-21. <https://doi.org/10.3354/ab00540>.
- 757 Saint-Amand, A., Lambrechts, J., & Hanert, E. (2023). Biophysical models resolution affects coral
758 connectivity estimates. *Scientific Reports*, 13(1), Article 1. [https://doi.org/10.1038/s41598-023-36158-](https://doi.org/10.1038/s41598-023-36158-5)
759 5
- 760 Šargač, Z., Giménez, L., González-Ortegón, E., Harzsch, S., Tremblay, N., & Torres, G. (2022).
761 Quantifying the portfolio of larval responses to salinity and temperature in a coastal-marine invertebrate:
762 A cross population study along the European coast. *Marine Biology*, 169(6), 81.
763 <https://doi.org/10.1007/s00227-022-04062-7>.
- 764 Seytre, C., Vanderklift, M. A., Bodilis, P., Cottalorda, J. M., Gratiot, J., & Francour, P. (2013).
765 Assessment of commercial and recreational fishing effects on trophic interactions in the Cap Roux area
766 (north-western Mediterranean). *Aquatic Conservation: Marine and Freshwater Ecosystems*, 23(2), 189-
767 201.
- 768 Sotelo, G., Morán, P., & Posada, D. (2008). Genetic Identification of the Northeastern Atlantic Spiny
769 Spider Crab as *Maja Brachydactyla* (Balss, 1922). *Journal of Crustacean Biology*, 28(1), 76-81.
770 <https://doi.org/10.1651/07-2875R.1>.

771 Steneck, R. S. (2006). Possible demographic consequences of intraspecific shelter competition among
772 American lobsters. *Journal of Crustacean Biology*, 26(4), 628-638.

773 Swearer, S., Treml, E., & Shima, J. (2019). *A Review of Biophysical Models of Marine Larval Dispersal*
774 (p. 325-356). <https://doi.org/10.1201/9780429026379-7>.

775 Torres, A., Dos Santos, A., Alemany, F., & Massutí, E. (2013). Larval stages of crustacean species of
776 interest for conservation and fishing exploitation in the western Mediterranean. *Scientia Marina*, 77,
777 149-160. <https://doi.org/10.3989/scimar.03749.26D>.

778 van Sebille, E., Griffies, S. M., Abernathy, R., Adams, T. P., Berloff, P., Biastoch, A., Blanke, B.,
779 Chassignet, E. P., Cheng, Y., Cotter, C. J., Deleersnijder, E., Döös, K., Drake, H. F., Drijfhout, S., Gary,
780 S. F., Heemink, A. W., Kjellsson, J., Koszalka, I. M., Lange, M., ... i a, J. D. (2018). Lagrangian ocean
781 analysis : undamentals and practices. *Ocean Modelling*, 121, 49-75.
782 <https://doi.org/10.1016/j.ocemod.2017.11.008>.

783 Vignoli, V., Caruso, T., & Falciai, L. (2004). Decapoda Brachyura from Monte Argentario
784 (Mediterranean Sea, central Tyrrhenian). *Crustaceana*, 77(2), 177-186.

785 Yin, J., Overpeck, J., Peyser, C., & Stouffer, R. (2018). Big jump of record warm global mean surface
786 temperature in 2014–2016 related to unusually large oceanic heat releases. *Geophysical Research*
787 *Letters*, 45(2), 1069-1078.

788 Zaimen, F., Ghodbani, T., & Vermeren, H. (2021). L'activité de pêche artisanale au sud de la
789 Méditerranée : Gouvernance, dynamique socio-économique et enjeux environnementaux dans le port
790 algérien de Jijel (Boudis). *VertigO-la revue électronique en sciences de l'environnement*, 21(1).

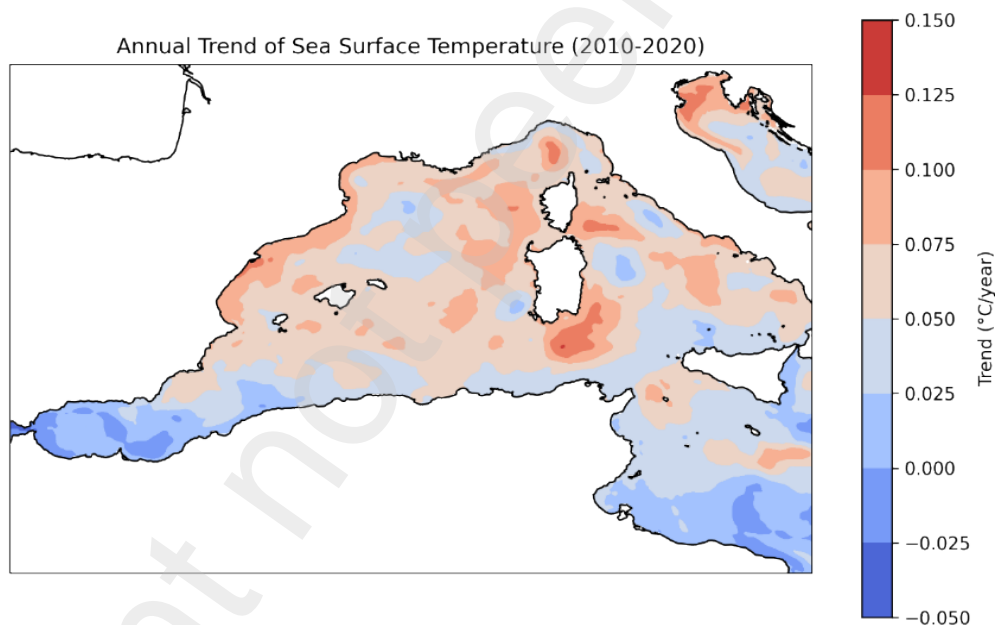
791 Zakardjian, B. A., Runge, J. A., Plourde, S., & Gratton, Y. (1999). A biophysical model of the interaction
792 between vertical migration of crustacean zooplankton and circulation in the Lower St. Lawrence
793 Estuary. *Canadian Journal of Fisheries and Aquatic Sciences*, 56(12), 2420-2432.
794 <https://doi.org/10.1139/f99-095>.

795
796
797
798
799
800
801
802
803
804
805
806
807
808
809
810

811
812
813

814 **Appendices**

815 The sea surface temperature data extracted from the Copernicus Marine Environment Monitoring
816 Service (CMEMS) satellite product over the western Mediterranean Sea demonstrated a temperature
817 increase trend of $0.034 \pm 0.002^{\circ}\text{C}$ per year, with a 95% confidence interval. To analyse trends spatially
818 and focus on the last decade, data from the Med MFC physical multiyear product (Mediterranean Sea
819 Physics Reanalysis) were examined at all points in the Western Mediterranean (focusing on our study
820 window). A linear temperature trend was calculated for each grid point based on time series data through
821 linear regression. A color gradient from blue (indicating a decrease in temperature) to red (indicating an
822 increase in temperature) was used to map these trends. The detailed analysis is presented in the figure
823 A1 below.



824
825 Figure A1: Sea Surface Temperature Trends in the Western Mediterranean from 2010 to 2020. This map illustrates
826 the decadal trend in sea surface temperatures, with the color scale ranging from -0.050°C (blue) to $+0.150^{\circ}\text{C}$ (red),
827 highlighting areas of temperature decrease and increase relative to the period average.
828